JOURNAL OF MATERIALS SCIENCE 31 (1996) 1969–1983

Grain size and porosity dependence of ceramic fracture energy and toughness at 22 °C

R. W. RICE
5411 Hopark Drive, Alexandria, VA 22310, USA

A review of the fracture energy and toughness data for dense ceramics at 22 °C shows maxima commonly occurring as a function of grain size. Such maxima are most pronounced for non-cubic materials, where they are often associated with microcracking and *R*-curve effects, especially in oxides, but often also occur at too fine a grain size for association with microcracking. The maxima are usually much more limited, but frequently definitive, for cubic materials. In a few cases only a decrease with increasing grain size at larger grain size, or no dependence on grain size is found, but the extent to which these reflect lack of sufficient data is uncertain. In porous ceramics fracture toughness and especially fracture energy commonly show less porosity dependence than strength and Young's modulus. In some cases little, or no, decrease, or possibly a temporary increase in fracture energy or toughness are seen with increasing porosity at low or intermediate levels of porosity in contrast to continuous decreases for strength and Young's modulus. It is suggested that such (widely neglected) variations reflect bridging in porous bodies. The above maxima as a function of grain size and reduced decreases with increased porosity are less pronounced for fracture toughness as opposed to fracture energy, since the former reflects effects of the latter and Young's modulus, which usually has no dependence on grain size, but substantial dependence on porosity. In general, tests with cracks closer to the natural flaw size give results more consistent with strength behaviour. Implications of these findings are discussed.

1. Introduction

Fracture energy (γ) and especially fracture toughness (K) have received much attention because of their basic role in fracture mechanics. This attention has been heightened by more recently emphasized concepts that focus on increasing toughness as a key route to greater reliability. This in turn has focused much attention on wake and related *R*-curve effects, which essentially show toughness being dependent on the extent of crack propagation. Of the two wake effects, transformation toughening and bridging, bridging has more recently received particular attention because of its potential broad applicability to both many polycrystalline and composite ceramics. Such wake, and related *R*-curve, effects have helped explain some of the differences between the different fracture energy/toughness tests. However, such effects still leave important differences between different tests unexplained, and raise other important questions, in particular the role of *R*-curve effects on strength, especially those due to bridging. The importance of these issues is compounded by recent, growing evidence that increased toughness does not necessarily result in increased reliability [1–4]. There are also considerable grounds for a closely related question, namely whether tests reflecting crack wake and resultant *R*-curve effects are directly related to strength behaviour [4].

Since there are many terms used repetitively, the abbreviations in Table I are used.

An important, but generally neglected, factor in resolving the above issues is the microstructural dependance of γ and K, and the correspondence of this with such dependence of flexure (tensile) strength (S) and Young's modulus (E). This paper reviews the grain size (G) and porosity (P) dependence of γ and K, primarily at 22 °C, providing a useful compilation of data and some insight into differences between different tests. However the primary purpose is to provide a counterpart to evaluations of the G [5–9] and P [9–11] dependence of S and E. While another paper addresses the differences between, and correspondences with, the G and P dependence of S and E [4], some observations on this are made in this paper. This paper significantly extends earlier reviews of the G dependence of γ [12, 13], reinforcing some of the trends observed there, but also showing possibly conflicting behaviour, and hence the need for further research. This paper also greatly extends an earlier, preliminary survey of the P dependence of γ [9, 14], and strongly indicates crack bridging or related phenomena occurring in some porous bodies. This has received almost no attention, but is probably important in the high resistance of some porous bodies to severe thermal shock, and thus should be a fruitful area for research.

0022–2461

TABLE I Terms and Abbreviations

Term	Abbreviation
(a) microstructure	
1. Grain Size	G
2. Porosity (Vol. fraction, or %)	P
(b) mechanical properties	
3. Strength (tensile or flexure)	S
4. Young's modulus	E
5. Fracture energy	γ[a]
6. Fracture toughness	K[a]
(c) Fracture energy/toughness tests	
1. Compact tension	CT
2. Double cantilever beam	DCB
3. Double torsion	DT
4. Fractography[b]	F
5. Indentation	I
6. Indentation fracture	IF
7. Notch beam[c]	NB
8. Work of fracture[d]	WOF

[a] The generic symbols (i.e. without the subscript IC) are used since it is not always clear whether the values are the critical ones controlling failure.
[b] Values derived from the failure strength and the flaw size, shape, and location detected on the fracture surface.
[c] Tests with a sharp crack introduced are noted.
[d] This includes all tests with a chevron notch.

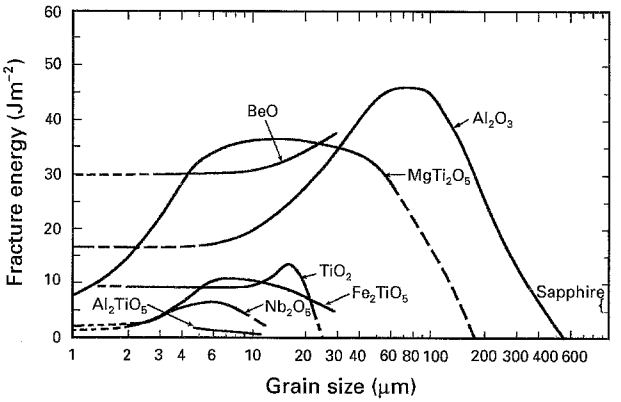

Figure 1 Fracture energy versus grain size (G) of non-cubic oxide ceramics at 22 °C. Curves and data points (for tests and sources shown) are average values from previous surveys [12, 13]. Note all data are shown for the average G, but some are also shown for the maximum G reported (via the horizontal bars).

2. Data review and discussion

2.1. Grain size dependence of fracture toughness of monolithic ceramics

2.1.1. Oxide ceramics

A previous study and review, primarily of oxides, showed that there was little or no G dependence of γ for cubic materials, but a substantial dependence for non-cubic materials [9–12]. Thus, γ of alumina, as measured by DCB methods, was shown to pass through a significant maximum at $G \sim 50$–100 μm (Figs 1 and 2). (Note that, unless there is some phenomena such as microcracking or phase transformation that depends on G, E does not depend on G. Therefore, the G dependence of K is similar to that of γ, moderated by $K \sim (E\gamma)^{1/2}$, so all further discussion of the G dependence will be in terms of K.) Results from various, more limited DT, WOF (i.e. chevron notch), IF, and NB tests are generally consistent with this G trend over the G range they covered, though there were often variations in the absolute values (Fig. 2). However there are variations in this and other data, some substantial, e.g. Hayashi *et al.* [15] showing WOF data reaching a slightly higher, substantially narrower, peak, but at $G \sim 20$ μm. K values of ~ 4 MPa m$^{1/2}$ in Figs 1 and 2 are also quite consistent with earlier [16] and more recent F [17, 18] K_{IC} values where flaw dimensions could be determined (typically for $G \sim 1/2$–10 μm), so long as the flaws are sufficiently large in comparison to G. A model based on the G dependence of microcracking from the thermal expansion anisotropy (TEA) of alumina and other non-cubic materials was developed to explain the G dependence of γ [19] of Rice and co-workers [12, 19] (Fig. 1).

Shortly following the above work, Claussen *et al.* [20] showed some literature and their own NB data starting at higher K levels at fine G and decreasing with increasing G. They attributed the significant rise to high values in DCB tests at larger G (Fig. 1) to microcracking, i.e. greater sensitivity to R-curve effects in DCB tests. Mussler *et al.* [21] extended this NB data (Fig. 2) and attributed the increasing K to an increasing notch sensitivity, i.e. that the true NB K values should be independent of G (at ~ 4 MPa m$^{1/2}$). They also showed K values from indentation fracture (IF) tests showing an almost identical increase to that for DCB tests over the G range tested (~ 1–35 μm), and assumed that both IF and NB results follow the decreasing trend of DCB results with G at larger G (i.e. beyond the DCB K maximum). Subsequent data [22–29], representative results of which are shown in Fig. 2, e.g. Hübner and Jillec [28] (see also Yokobori *et al.* [22]) show a very similar K decrease with increasing G for NB tests as Mussler *et al.*, but K increasing with G when tests were made on beams with a sharp crack instead of a fine notch. Also note that Veldkamp and Hattu's [29] data showing no G dependence used an indentation to introduce a sharp crack at each end of the notch in their NB test.

The increase in K with increasing G is now commonly attributed to crack bridging and associated R-curve effects, which have been widely demonstrated to occur in alumina [19, 30–34]. While actual bridging observations are typically made in DCB or compact tension (CT) tests, effects of bridging, i.e. R-curve effects, have now been demonstrated in essentially all of the fracture mechanics tests (other than fractography). Thus, while the initial K, i.e. without R-curve effects, shows little or no G dependence, bridging and resultant (large crack) toughness increase with G (at least over the modest G range of such tests, e.g. to $G \sim 30$ μm) [31]. The extent of bridging and its interaction with the decrease in K as G increases at large G has not been examined.

Turning now to other non-cubic oxides, previously summarized BeO WOF and DCB data [12, 13] show the start of a similar G dependence of alumina over the G range tested (Fig. 1). WOF data of Cleveland [35] for $MgTi_2O_5$, Fe_2TiO_5, and Al_2TiO_5 also show

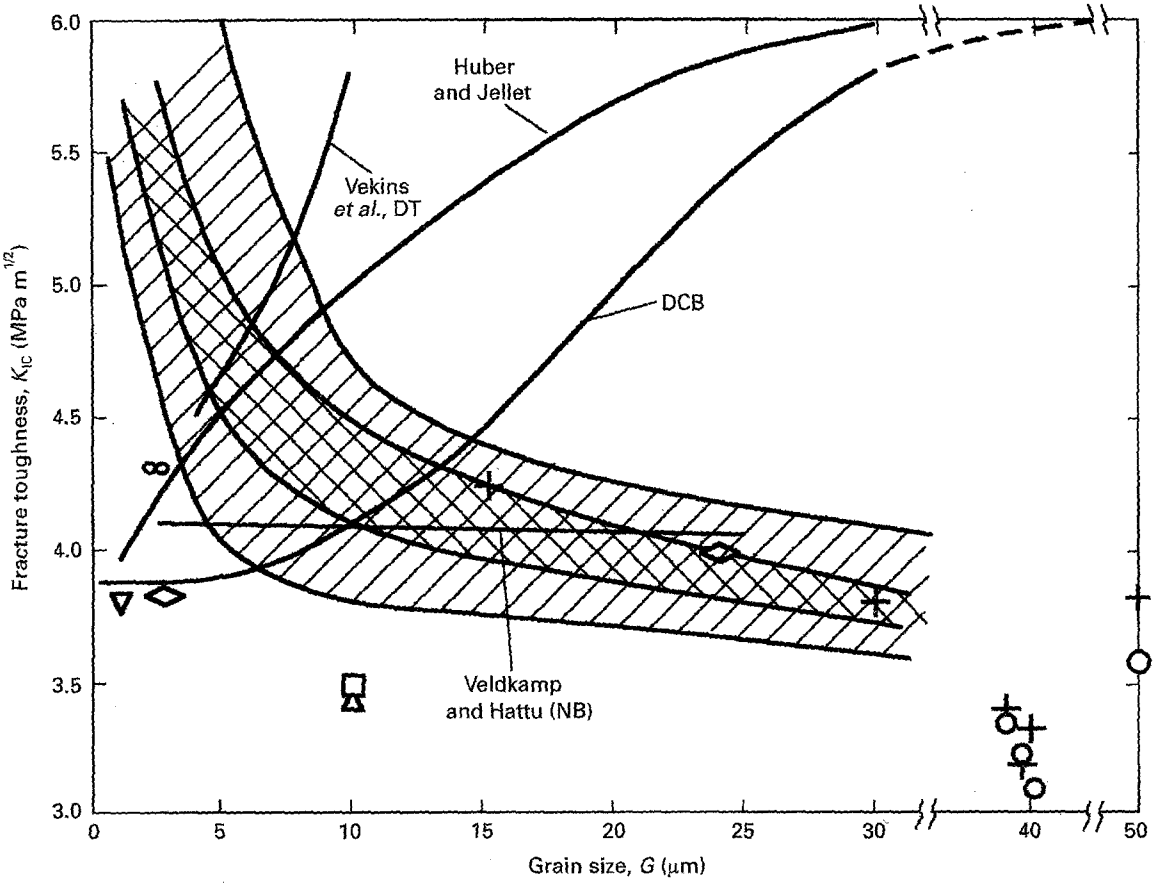

Figure 2 Fracture toughness (K) of Al_2O_3 versus G at 22 °C. The DCB data of this author and colleagues [12] and of Veldkamp and Hattu [29] from Fig. 1 are shown along with data of other investigators and tests [24–29], as listed. Key: ////// Mussler *et al.*, NB; \\\\\\ Huber and Jellet, NB; ▽ NB, Nishida *et al.*; △ NB, Munz *et al.*; □ WOF, Munz *et al.*; ∞ DT, Sclosa *et al.*; ◇ NB, Sclosa *et al.*; ○ NB, Yank *et al.*; + IF, Yank *et al.*

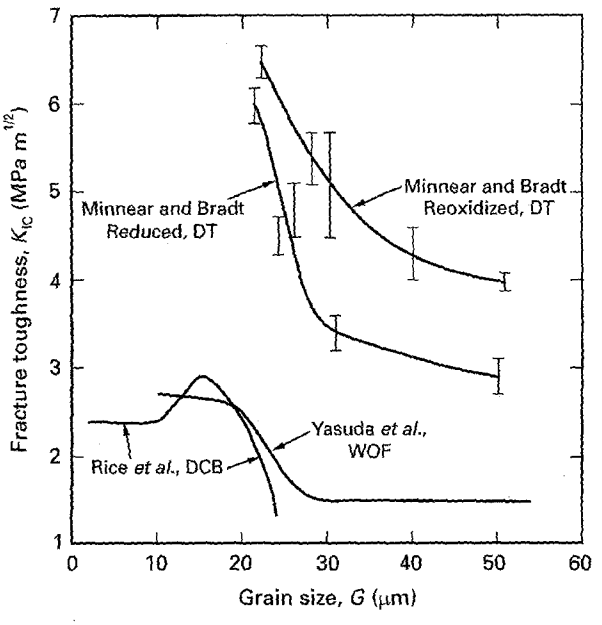

Figure 3 Fracture toughness (K) of TiO_2 versus G at 22 °C. The DCB data of this author and colleagues from Fig. 1 along with data of Minnear and Bradt [37] and of Yasuda *et al.* [38] are shown. Note that, while the absolute values of the latter investigators are substantially higher, all data shows a substantial decrease in K_{IC} occurring by or before $G \sim 20$ μm.

γ maxima (Fig. 1), and Pohanka *et al.* [36] have further shown a K maximum (~ 1.8 MPa m$^{-1/2}$ at $G \sim 40$ μm) in DCB tests of PZT. Minnear and Bradt's [37] DT data showed as hot-pressed TiO_2 with much higher K values than Rice *et al.* [12], but both were consistent with a sharp K decreases by $G \sim 20$ μm (Fig. 3). It is also consistent with, but does not confirm, a K maximum at $G < 20$ μm or less. Their reoxidized TiO_2 shows a somewhat higher K and slower decrease with increasing G, but is consistent with the above observations. Yasuda *et al.*'s WOF data for sintered TiO_2 [38] is very consistent with the decrease of K as G increases above 15–20 μm, but leaves the existence of a K maximum at $G \sim 15$ μm uncertain. They also showed essentially the same decrease in E, thus strongly supporting the attribution of the K decrease to microcracking from TEA stresses, and consistent with other estimates for the G onset of microcracking [39].

Consider next data for cubic oxides as summarized in Figs 4 and 5. Previous WOF data of Kessler *et al.* [40] for transparent, hot-pressed MgO, which was consistent with limited DCB, as well as NB tests for similar MgO, showed no dependence on G. This is quite consistent with WOF data of Yasuda and colleagues [41–44] for dense, hot-pressed MgO, with or without oxide additives. These additives, typically at the 10% level, modestly increased the K level, but left it independent of G over the range studied (Fig. 4). Two results of Kessler *et al.*'s study should be noted. First, γ of MgO, as hot-pressed with LiF additions was $\sim 1/2$ that of specimens annealed to remove most, or all, of the LiF remaining after hot pressing, or made without LiF. Thus, the presence of residual LiF

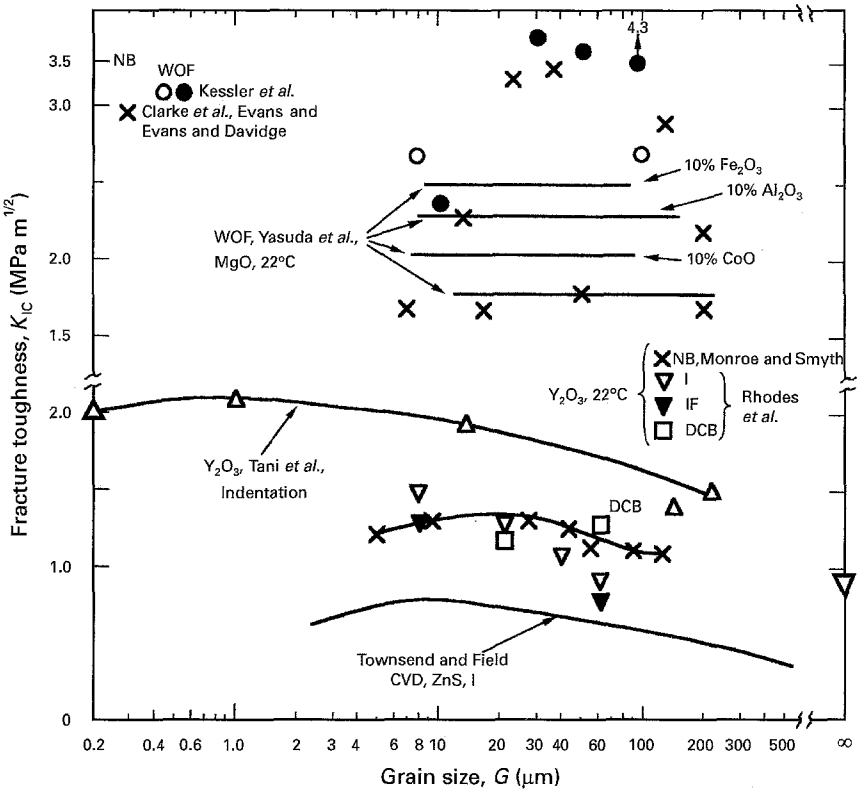

Figure 4 Fracture toughness (K) of MgO, Y_2O_3, and (CVD) ZnS versus G at 22 °C. MgO data (upper plot) from a previous [39] and more recent [40–43] study of pure and doped MgO shows no G dependence for bodies with ~0% porosity $< (P)$. However, MgO with $0.1 < P < 1\%$ (solid circles) clearly increased K_{IC} with increasing G as P decreases and shifts to a more intragranular character. The typical K_{IC} for {1 0 0} fracture of MgO crystals is 1 ± 0.2 MPa $m^{1/2}$ [44]. The Y_2O_3 data are for three studies [45–47] and various tests as shown. Note the single crystal value for Y_2O_3 at far right. The ZnS data are for CVD material [78].

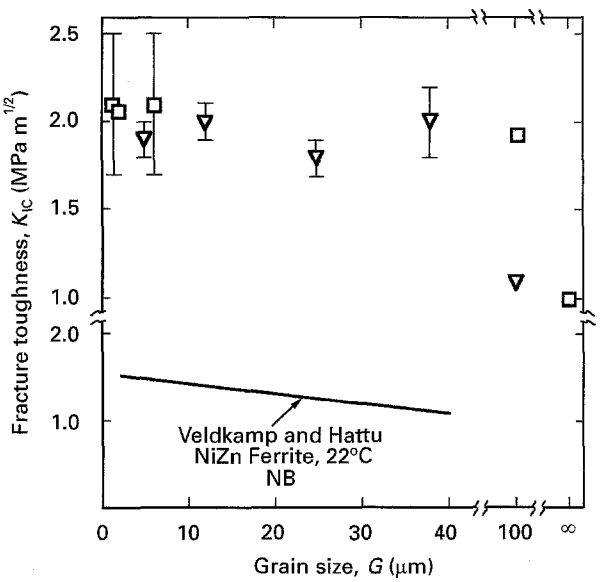

Figure 5 Fracture toughness (K) of $MgAl_2O_4$ and a NiZn ferrite versus G at 22 °C. Note the good agreement (▽, IF) (□, DCB) between data of Stuart *et al.* [52] and Rice *et al.* [12] for material without additives, the much lower value for $MgAl_2O_4$ made with LiF, and the value for fracture on either {1 0 0} or {1 1 0} single crystal planes. The ferrite data are from Veldkamp and Hattu [29].

(which was associated with 100% intergranular fracture versus substantial transgranular fracture otherwise for the same grain sizes) reduced K by about 30%. Second, the presence of limited porosity resulted in K increasing with G (discussed further later on). Also note K for {1 0 0} MgO single crystal cleavage is ~ 1/2 that of the polycrystalline K [45].

Monroe and Smyth's [46] NB results for sintered Y_2O_3 ($P < 4\%$) showed a probable limited K maximum at $G = 10$–30 μm, or at least a K decrease at larger G (Fig. 4). Their results are in good agreement with limited I, IF, and DCB data reported by Rhodes *et al.* [47] for their Y_2O_3 sintered to transparency. Tani *et al.*'s [48] indentation K values for fully dense (hot-pressed) Y_2O_3, though substantially higher than those of Monroe and Smyth, are also consistent with a possible K maximum, but at a much finer G (~ 1 μm). Their data clearly support K decreasing with increasing G above ~ 15 μm.

Earlier DCB [12] and more recent IF [49–52] data for dense $MgAl_2O_4$ (made without densification aids) show excellent agreement and no dependence on G (Fig. 5). K values from F agree very well with the results of Fig. 5 for $G \sim 3$ μm [17] and for $G \sim 100$ μm (provided that the flaw size was $> G$) [17]. Stuart *et al.*'s [52] report of ~ 40% lower K for $MgAl_2O_4$ (hot pressed with LiF, Fig. 5), with essentially all intergranular fracture, should be noted in contrast to very predominant transgranular fracture in $MgAl_2O_4$ made without additives [52, 53]. This effect of residual boundary additives is very similar to MgO results noted earlier, and is of particular note, as discussed further later on, since $MgAl_2O_4$ made with LiF shows substantial bridging [49, 50]. Also shown in Fig. 5 is the data of Veldkamp and Hattu [29] for a dense Ni Zn ferrite using their NB test with indent cracks at each

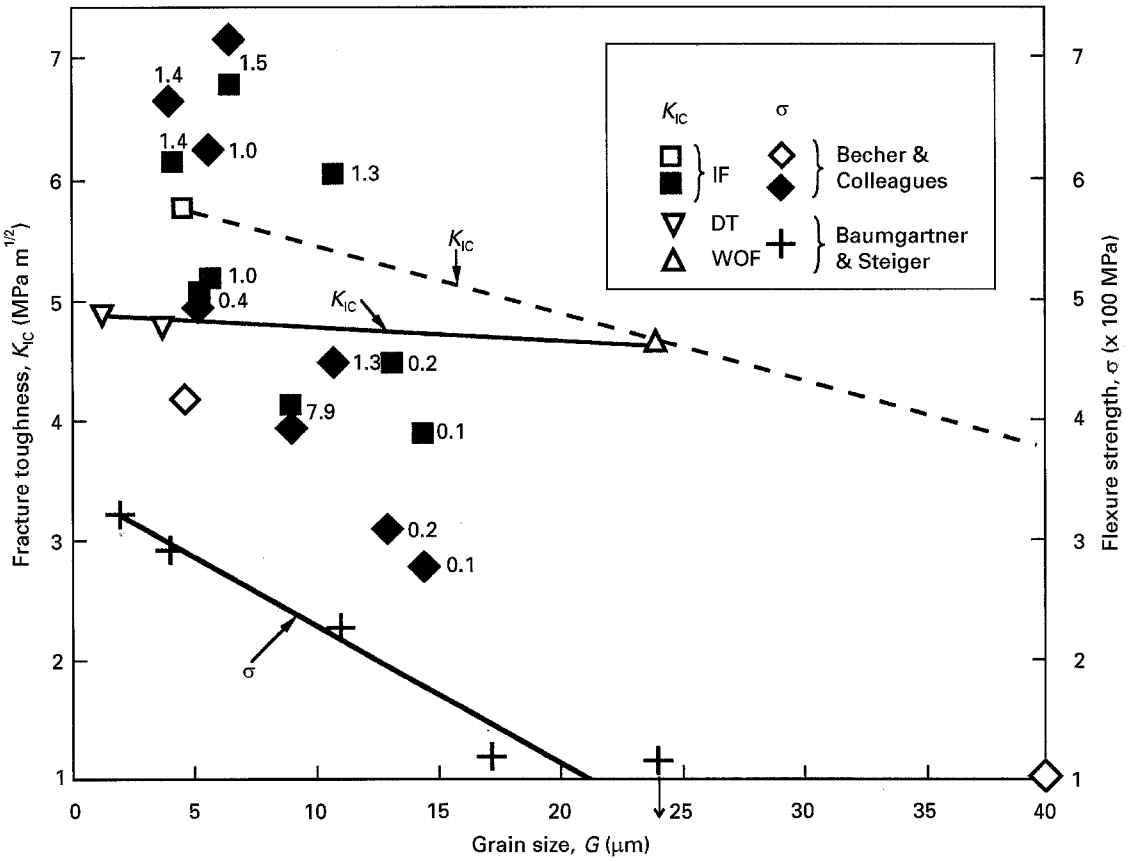

Figure 6 Fracture toughness (K) and strength of TiB_2 versus G at 22 °C. Data of Baumgartner and Steiger [54] and of Becher and colleagues [55, 56], the latter without Ni additions (open symbols) or Ni additions (solid symbols, % Ni shown next to each datum point).

end of the notch. They noted that changes in residual impurities and stoichiometry as G changes might be factors in the ~ 15% decrease from $G = 30$ to 40 μm.

2.1.2. Non-oxide ceramics

DT and WOF data of Baumgartner and Steiger [54] for sintered TiB_2 ($P \sim 0.5$–1.5%, $G \sim 1.4$ and 24 μm) show K decreasing ~ 5% as G increases (Fig. 6). Indent, and IF K data of Becher and colleagues [55, 56] for TiB_2 hot pressed with, or without, Ni ($P = 1$–2%, $G = 4$–40 μm) agree reasonably well with the DT–WOF data, except showing a substantially greater (~ 25%) decrease as G increases. The addition of Ni tended to increase K, at least at finer G, but still showed K decreasing with increasing G, quite possibly faster than without Ni. Results of Kang *et al.* [57] for TiB_2 with 5–2% B_4C + 0.5% Fe ($G \sim 4$ μm, $P \sim 4$%, $K_{IC} \sim 5.5$ MPa m$^{1/2}$, $S \sim 400$ MPa) and Matsushita *et al.* [58] for TiB_2 with 7.5% (14 Ni : 1.5C) ($G \sim 5$ μm, $P \sim 1$%, $K \sim 4.8$ MPa m$^{1/2}$, $S \sim 470$ MPa) are in good agreement.

DCB data of this author and colleagues on a variety of hot-pressed B_4C materials from several sources ($P = 0.4$–2.8%) indicates K rising to a maximum or plateau at $G \sim 7$–10 μm (Fig. 7) [59]. Korneev *et al.* [60] show a very distinct K maximum at $G = 10$ μm in their NB tests of hot-pressed B_4C. Niihara [61] and Niihara *et al.* [62] also report pronounced maxima of both Vickers hardness and indent K for their B_4C made by chemical vapour deposition (CVD) at stoichiometry, i.e. a B/C ratio of ~ 4. The decrease in K values at lower B/C ratios was attributed to excess C at the grain boundaries, and at higher B/C ratios (where the decrease was corroborated by two DCB tests) to reduced bond strength as the B content increased, and not to the variation in G (2–20 μm) or the limited P. However note that their data are in good agreement with the other data based on the fact that their K peak at B/C = 4 was apparently at $G \sim 5$–10 μm, and the assumption that G became smaller as the B/C ratio increased or decreased, and became larger for the opposite change in B/C ratio. There is a clear precedent for this. Kalish *et al.* [63] reported Knoop hardness of dense B_4C hot pressed to B/C ratios of 3.7–5.1, tending to decrease as the B/C ratio decreased, but with substantial scatter. However, Rice *et al.* [64] subsequently showed that the primary factor accounting for the substantial hardness change was the change in G due to the variations in the B/C ratio, and not the ratio itself, i.e. at constant G variations of B/C had only limited effects on hardness. Calculations from flexural strengths and flaw geometry from fractography of B_4C with average G of 2, 5, and 10 μm gave $K = 3.4 \pm 0.5$ MPa m$^{1/2}$ [65], i.e. in good agreement with the average value in Fig. 8.

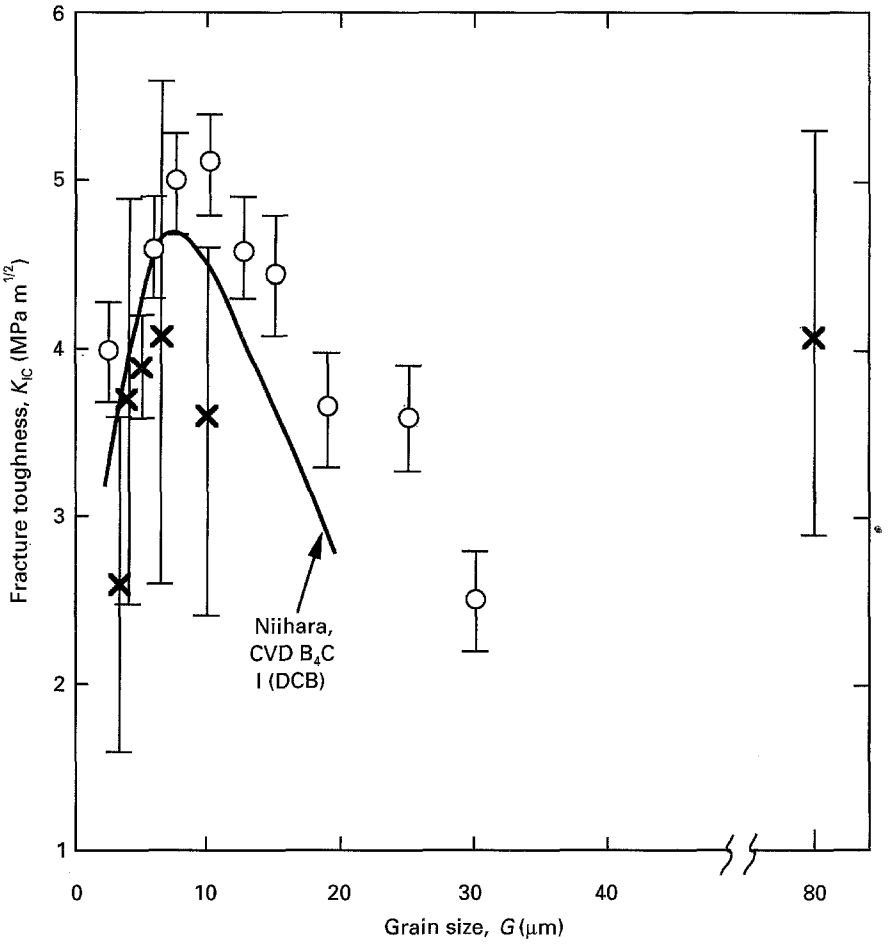

Figure 7 Fracture toughness (K) of B_4C versus G at 22 °C. Data of Rice and colleagues [59] (X, DCB) and Korneev *et al.* [60] (○, NB) for hot-pressed material along with that of Niihara and colleagues (for CVD material) [61, 62]. Note that the large G datum point is for material with a few to several % P, and hence may be high as discussed in the text.

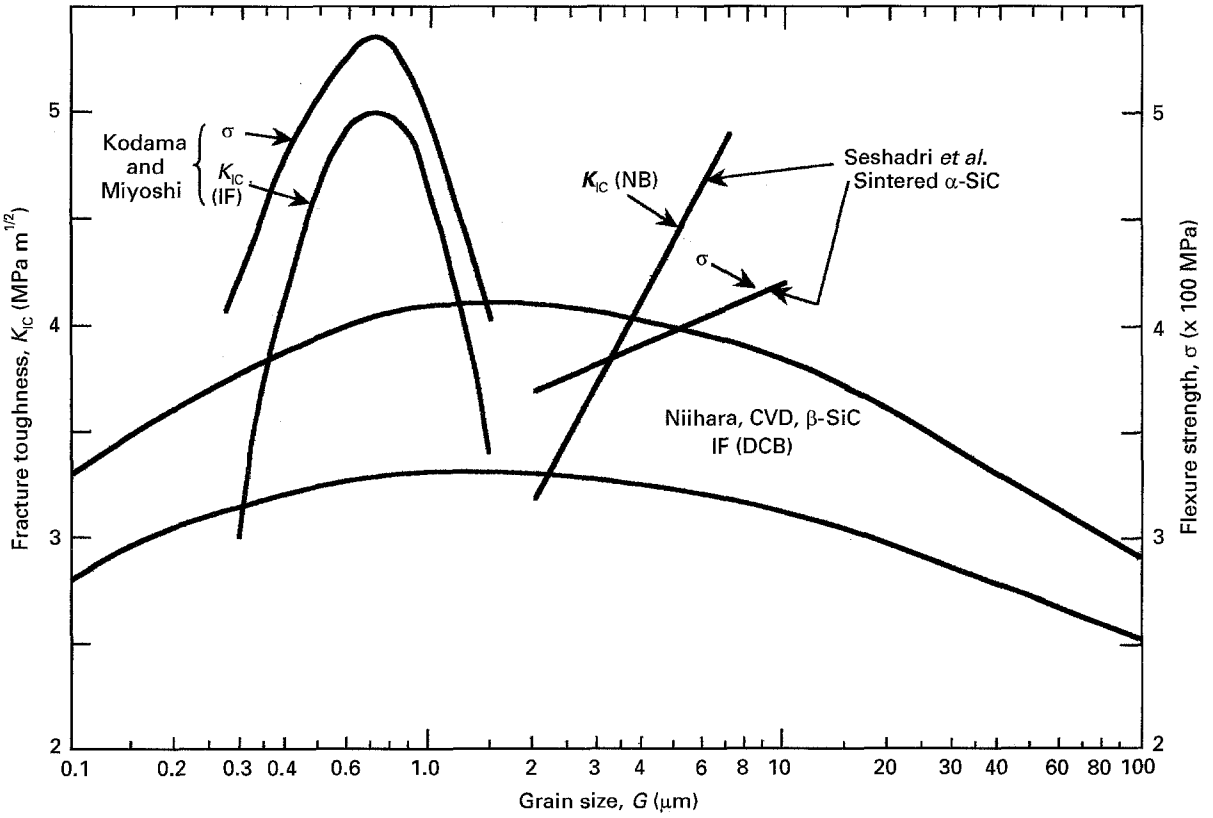

Figure 8 Fracture toughness (K) and strength of SiC versus G at 22 °C. The data of Kodama and Miyoshi [66] is for polycarbosilane derived SiC (note this is a rare case of a strength maximum versus G), Niihara [61] for CVD SiC, and Seshardi *et al.* [67] for sintered alpha-SiC.

Niihara [61] also reported indent K for CVD (beta) SiC showing a distinct maximum at $G \sim 1$–3 μm (Fig. 8). The maximum K value was also corroborated by limited DCB tests. Kodama and Miyoshi [66] reported a more pronounced indent K maximum at $G = 0.7$ μm for their polycarbosilane derived, hot-pressed SiC (Fig. 8). Whether the lower K values at the finer or larger G, and the maximum, are due just to their G, or to their specimens being either mainly beta- or alpha-SiC, is not certain. However, values for both types of SiC agreed at $G \sim 1 \pm 02$ μm. Seshadri *et al.*'s [67] NB tests for sintered alpha SiC showed a marked ($\sim 33\%$) increase in K over the limited G range (2–7 μm) tested. On the other hand, fracture energies from an earlier survey [12], reflecting WOF, DCB, and NB tests, for G mainly 10–100 μm by themselves showed no obvious G dependence, but are not inconsistent with the data of Fig. 8, i.e. being in the range of $K = 3.5$–5 MPa $m^{1/2}$. However, Seshadri and Srinivasan's [68] fracture analysis of sintered alpha-SiC (failing mostly from isolated pores) indicates K of only 2–3 MPa $m^{1/2}$, which is in good agreement with similar analysis by Ohji *et al.* [69] and their NB K of 2.3 MPa $m^{1/2}$.

Extensive measurements by many investigators using a variety of techniques on various dense Si_3N_4 materials typically give $K = 4$–6 MPa $m^{1/2}$ for G of a few microns [45, 70–74]. Values toward the lower end of this range are typically obtained from fractography, i.e. from observed flaw geometry and failure stresses. Higher values, e.g. to ~ 11 MPa $m^{1/2}$, are associated with larger, but elongated, grains, and significant R-curve effects [73–74]. However, starting toughness of such materials showing R-curve effects, i.e. before significant crack propagation, are commonly still in the 4–5 MPa $m^{1/2}$ range. These trends are corroborated and systemized by the work of Kawashima *et al.* [75] showing K continuously increasing from 5.4 to ~ 11 MPa $m^{1/2}$ as G increased over the range of G investigated (2.4–10 μm), suggesting that K passes through a maximum as a function of G. Data of Hirosaki *et al.* [76] on *in situ* toughened Si_3N_4 showing K passing through a maximum of ~ 10.3 MPa $m^{1/2}$ as G of their mixed microstructures increased from ~ 0.2–2 μm diameter and 1–5 μm long to 2–20 μm diameter and 10–100 μm long corroborates this. These studies, and others outlined above, indicate that the K maximum occurs in the G range of 10–20 μm, e.g. based on a K maximum of 10–20 MPa $m^{1/2}$. Such a G range for a K maximum is not necessarily inconsistent with microcracking from thermal expansion mismatches [38] within the alpha ($\sim 0.1 \times 10^{-6}$/C) and beta ($\sim 0.5 \times 10^{-6}$/C) phases [77a], and between these and the grain boundary phase(s).

Townsend and Field [78] reported a distinct maximum in their indent K values for CVD (cubic) ZnS (Fig. 7, which was coincident with a distinct hardness minimum).

2.2. The Porosity dependence of fracture energy and toughness

The P dependence of the mechanical properties of ceramics, though not receiving much attention, are very important in an overall understanding of mechanical behaviour of ceramics and other brittle materials. They are particularly pertinent to this paper since, while strength and toughness show some common trends, there are also important differences in their P dependence. The P dependence of S and E, for which there is much more data than for γ or K, which has recently been reviewed [10, 11], provides useful background. Both S and E show a continuous decrease with increasing P that is initially approximately linear on a semilog plot of S versus P, but then progressively decreases more rapidly to then fall precipitously to zero as the porosity for the percolation limit for the solid phase (P_C) for the particular type of porosity is reached. Of these characteristics, the slope of the approximately linear semilog property dependence from $P = 0$ up to 1/3–1/2 of P_C is the most unique to a given porosity, and is most pertinent to most of the cases of interest, and is hence of central interest here. This slope is often expressed as the b value in $\exp(-bP)$. Such P dependence is consistent with predictions of minimum solid area models, which predict b values of 3–5 for most pore structures (but values down to 1 + and up to 9 are seen), and are consistent with an extensive survey of the P dependence of strength and E (as well as of thermal and electrical conductivity) [10, 11].

In evaluating these trends, it is important to consider the P dependence of both γ and K since E has substantial dependence on P. Thus, K, for which there is more data, reflects effects of P on both E and γ. This is in contrast to effects of grain (or particle) size, which generally have little or no effect on E, so their effects on γ are reflected in their effects on K as discussed earlier. Most individual studies of the γ or K dependence on P do not also entail measurements of S or E, let alone both, thus requiring comparison with average trends from other studies. However, there are a few studies in which most, or all, of these properties have been made on the same set of samples, thus giving direct comparison between tests in addition to comparison of overall trends. There are clear cases of the P dependence of γ or K (or both) being quite similar to that of E or S (or both), including common tests from the same study [79, 80] (Table II). Close similarity of γ or K and E, S, or both, are also shown by the normalization of K (or γ) values calculated from fractography of bodies of varying P to the corresponding values at $P = 0$ using the same b value found for the P dependence of S of Al_2O_3 and B [18]. The similarity of some P dependence of γ and K with E and S is also shown in some of the examples shown below.

There are, however, significant departures from the overall correspondence of S and E with K and especially γ dependence, of P. Some of these differences are fairly extreme, as discussed below. Two cases [82, 83] of higher apparent P dependence of K (i.e. similar to, or somewhat higher, than that of) S or E are due in part to variable G with P; i.e. finer G at higher P and the increase in S with decreasing G. There is thus a very common trend for a lower P dependence of K, and especially γ, similar to the more extreme cases,

TABLE II Comparison of the porosity dependence of fracture energy (γ) and toughness (K) with that of Young's modulus (E) and tensile strength (S)

Material	Fab.[a]	G[b] (μm)	P[c] (%)	Slope[d] (b value) for γ		K	E	S	Investigator
Al_2O_3	PC	0.5	~ 4–42	3.3	(NB)	3.4	3.4	3.4	Lam *et al.* [79]
Al_2O_3	HP	~ 1	~ 2–40	1.5	(DCB)	2.2	2.6	–	Wu and Rice [80]
Al_2O_3	HP	~ 1	~ 0–9	0	(WOF)	2	–	–	Cappola and Bradt [81]
Al_2O_3	S	< 5–50	~ 0–44	~ 3	(NB)	~ 3.4[e]	2	–	Pabst [82]
Al_2O_3	HP/S	~ 2–20	~ 2–46	–	(NB)	< 4.2[e]	2.1	–	Claussen *et al.* [83]
Al_2O_3	S	3	~ 5–50	–	(SEPB)	2.5	–	2.9	Evans and Tappin [84]
PZT	S	–	~ 2–15	–	(DT)	2.4	2.6	3.4	Biswas and Fulrath [85]
B_4C	HP	5	~ 0–15	–	(DCB)	2.3	2.7	3.9	Wu and Rice [80]
B_4C	HP	5	~ 0–15	0	(DT)	3.4	–	–	Hollenberg and Walther [86]
Si_3N_4	HP/S	~ 2–4	~ 0–10	–	(I)	5.2	5.4	–	Mukhoyadhyay *et al.* [70]
Si_3N_4	HP/S	~ 2–4	~ 0–50	–		2.4	3.7	4	Rice *et al.* [72]

[a] Fabrication: PC = pressure cast (and sintered = S), HP = hot pressed.
[b] Grain size.
[c] Porosity.
[d] Slope of approximately linear region of property on a semilog plot versus P at low to intermediate P level.
[e] Finer G at higher P is a major reason for higher b values for K than E.

indicating broad deviations of the P dependence of K, and especially γ, from that of E and S. This lower P dependence of γ and K versus those of E and S is also shown in Table II. It is also shown by the P dependence of K for bodies of sintered ZrO_2 bubbles being less than other mechanical properties [87], which was found by comparing data for highly porous materials [10], and is seen in comparing broader P trends from tests on different materials. This trend for lower P dependence of K is consistent with the frequent lack of normal P dependence of γ discussed below. It should also be noted that the PZT data of Table II is for bodies where much of the porosity was left from burnt out latex spheres [85]. The resultant spherical pores acted as fracture origins but were too far apart to have led to bridging effects on S [88].

While some of the limited γ–P data generally follow the overall P trends for other mechanical properties [14] discussed above, there are important deviations. Thus, Cappola and Bradt [81] reported that γ (from WOF tests) of hot-pressed Al_2O_3 was constant at $\sim 12\,J\,m^{-2}$ over the range studied ($P = 0$–0.1). Similarly Hollenberg and Walther [86] reported γ from DT tests of hot-pressed B_4C was constant at $\sim 3.3\,J\,m^{-2}$ over their P range (0–0.15). However, they showed a normal P dependence of E ($b \approx 3$) for this material, as well as a normal strength dependence ($b \approx 4$), both confirmed in separate tests [80] of the same material. The latter tests also showed a P dependence of K (in DCB tests) having $b \approx 2$, i.e. lower than for E and strength. The lower P dependence of K is consistent with a low P dependence of γ and a normal P dependence of E. Little, or no, P dependence, or possibly a temporary increase, of γ at lower P was also shown by Case and Smyth [89] in their NB tests of sintered Gd_2O_3 to $P = 0.15$, but then showed a normal decrease as P increased to 0.5, i.e. $b \approx 4$ (Fig. 9). This author and colleagues [59] have observed the lack of a decrease, and possibly a temporary increase in DCB K tests of porous hot-pressed MgO and Al_2O_3 (Fig. 9), i.e. more extreme than the lack of γ decrease noted above in some materials at $P < 0.15$.

There can also be opposite trends with coupled P and G changes at low P, e.g. as shown for MgO with low P. The increase in toughness from approximately the typical values for dense bodies with P decreasing and shifting from intergranular fracture toward more intragranular character as G increases (Fig. 4) is in good agreement with data of Clarke *et al.* [90]. There, K values, similar to those for fully dense bodies at finer G, were for the higher levels of P (~ 2.7%, mostly intergranular), and higher K values were for the lower P (~ 0.5%, much of which was intragranular).

Significant deviations can also occur at higher P. Thus, in γ studies of Si_3N_4, some porous bodies were found which had γ values well above the normal decrease with P, with some γ values for $P = 0.45$–$0.65 \geqslant$ to those for $P = 0$ [13, 72]. Microradiographic examination of the porous high γ samples showed crack branching and bridging due to interaction with the (artificially introduced, approximately spherical, ~ 100 μm diameter) pores. Such crack phenomena were not observed in specimens not showing significant γ–P deviations. The overall K–P trend was a continuous decrease with increasing P, but with a lower b (slope) than for E or strength (Table II), but there was no effect of the high γ values on strength. The microradiography showed that the crack bridging and branching phenomena were on a scale far larger (e.g. hundreds to thousands of microns) than the scale of flaws causing failure. Thus, the branching and bridging occurred with large cracks used for γ/K measurement either did not occur with strength controlling flaws, or occurred with them only after failure had essentially occurred; i.e. after catastrophic failure was already assured. Osipov *et al.* [91] also reported the NB K of B_4C to decrease from 4.6 to 2.8 $MPa\,m^{1/2}$ as P increased from 0 to ~ 0.12, then remained constant to $P \sim 0.28$ before again decreasing as P increased further. Less P dependence of K at medium and high P are also shown in model specimens of sintered glass beads and in foam materials [11].

Bridging can be seen as a natural consequence of two aspects of porous materials. The first is to provide

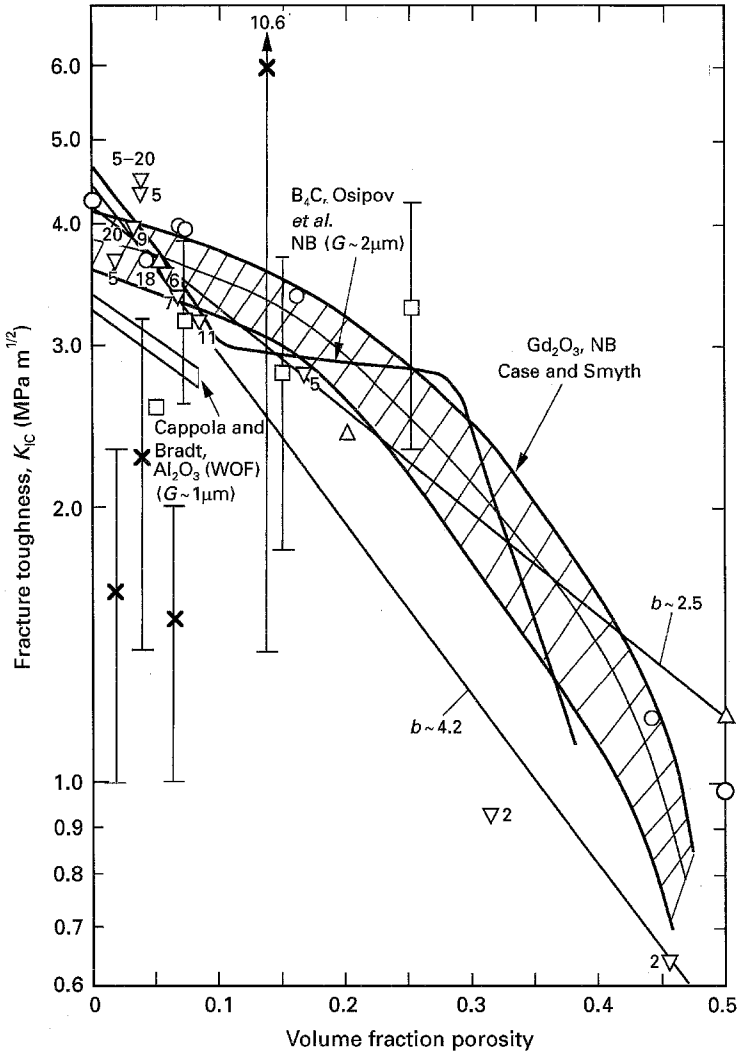

Figure 9 Fracture toughness (K) of Al_2O_3 [58, 82–84], Gd_2O_3 [89], MgO [58] and B_4C [91] versus P at 22 °C. Note broad variations in the P dependence of K, e.g. some due to initially no, or a reverse, dependence of γ on $P < 0.1$–0.15, respectively, for Al_2O_3 and Gd_2O_3. However, even broader variations are seen in Al_2O_3 and MgO data of this author and colleagues [59]. Some Al_2O_3 data show higher b values closer to or greater than the P dependence of S and E, but is due in part to G variations. Note the contrast in the P dependence of B_4C from Osipov *et al.* [91] to that of Wu and Rice [80] and Hollenberg and Walther [86] (the latter two are essentially identical and were measured on the same set of samples, Table II). Note similar contrast in Si_3N_4 data of Rice *et al.* [72]. Key: Al_2O_3: ▽ Claussen *et al.*, NB (G as shown); Δ Evans and Tappin, NB ($G \sim 3$ μm); ○ Pabst, NB ($G \sim 10$–50 μm); □ NRL, DCB ($G < 1$ μm): MgO: X DCB, NRL ($G \sim 1$ μm).

intrinsic alternative fracture paths in ideal porous structures due to cracks seeking two aspects of their paths, namely to fracture the minimum amount of solid (i.e. to propagate through more porous areas), but to also propagate approximately normal to the applied stress. This readily results in alternative crack paths for ideally stacked particles or pores (Fig. 10). Such alternative crack paths are likely to result in bridging when one path is, at least temporarily, incomplete, e.g. due to modest differences in local crack propagation. The second factor is heterogeneity of porosity, which may operate on much larger scales than the intrinsic effects of pore stacking. Clearly both can interact, which would extend both the scale and frequency of occurrence.

Bridging and branching effects with large, but not small, cracks would explain the common deviations of γ and K from tests with large cracks to have less P dependence than strength, which has similar P dependencies to that of E. It would also explain the higher resistance of porous refractories to severe thermal shock [13]. Thermal shock resistance is typically proportional to strength divided by the product of E and the thermal expansion coefficient. Thus, the similar, or identical, P dependence of E and S leave totally unexplained the large improvements in resistance to failure from severe thermal shock commonly resulting from porosity. This disparity is increased in the many cases in which thermal shock resistance is also proportional to thermal conductivity, which decreases with increasing P. However, since thermal shock of quite porous bodies is likely to involve propagation and arrest of larger cracks, the resultant bridging and branching noted above with large cracks and resultant lower dependence of γ and K versus that of E in many porous bodies could well explain their highly improved thermal shock resistance. Thus studies of crack bridging and branching of porous bodies should be a fruitful area for study.

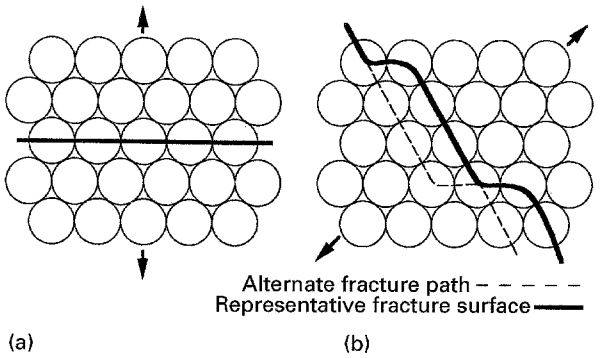

Figure 10 Schematic of crack branching–bridging in ideal porous materials: (a) shows fracture of a body of stacked balloons stressed along ⟨1 0 0⟩ axes where there is no opportunity for branching; (b) shows the same body stressed in another direction where the crack seeking to compromise between fracturing the least material while staying as close as possible to being approximately normal to the applied stress, leads to alternate branching paths.

3. General discussion

3.1. Measurement issues

Two factors need to be considered in comparing various tests. The first, and most obvious is each γ or K test, and how its results may be affected by test parameters. This is a large topic that has received considerable attention in developing these tests, though still leaving many differences incompletely understood. Several issues pertain mainly, or exclusively, to NB tests. Such tests have been shown to need a sufficiently fine notch root radius (e.g. < 10 μm) to give valid results. Whether such radii give valid results for all microstructures, not just the typical low to zero porosity, moderate to fine grain, (mostly alumina) specimens commonly investigated, needs further study. The reversal of the K–G trend depending on whether or not there was a notch or a sharp crack was used (Fig. 2) reflects this need. A basic factor in the NB test that is seldom checked is whether there is a sharp crack of sufficient length along the notch to be consistent with the assumption of a slit crack. This assumption can be violated, giving higher K values by up to ~ 2, consistent with fracture initiating from an approximate halfpenny rather than a slit crack, as shown by fractography of glass [92] and ZrO_2 crystals [93]. In the glass samples failure from cracks closer to halfpenny instead of slit cracks was more common in larger samples, giving an apparent specimen size effect [92].

Issues for other, especially indent and DT, tests are outlined as further examples. For indent methods, residual stresses from the indent, which depend on indent type and load, as well as material and microstructure, and whether these are removed by annealing or machining off the indent, is an issue, as is crack irregularity, which also depends on material parameters and G [94]. For DT tests the location of the groove relative to the loading direction, i.e. whether it is on the specimen top or bottom may be an issue [86].

A broader issue regarding γ and K measurements is the extent to which R-curve and bridging affects the tests and the extent to which these pertain to strength behaviour. While all of the widely used fracture mechanics tests can exhibit such effects, the extent of this depends on various factors such as grain size and the extent of crack propagation and crack shape. Effects of crack shape occur if wake effects such as bridging occur since the rate of change of crack wake area is greater for test specimens with curved (e.g. F, IF, I, and DT) versus straight crack fronts (e.g. CNB, NB, and DCB) [95].

There is clearly a dependence of K on the extent of crack propagation where there is significant wake effect, i.e. with phase transformation or bridging. Though apparently not examined, the effect of the extent of crack propagation implies a dependence on starting crack size, since crack propagation is usually involved in developing the "starting crack". Specific crack sizes are identified in the fractographic (F), indentation fracture (IF), and indent tests (I), with the crack size generally increasing in the order listed, especially from the F to the IF test. While specific crack sizes (both depth into the specimen and length or crack front periphery) are normally not identified in CNB, NB, DCB, and DT tests, these generally have increasing crack sizes in the order listed with sizes starting from, or above those of IF, and I tests. Examination of literature data (Table III) [96–104] where investigators measured K by two or more methods show a trend for K to increase with the indicated order of expected crack size. Thus, K values from fractography, which clearly involves the smallest cracks, are similar to, or somewhat less than, those from IF, I, etc. tests, while higher values are seen with DCB, and especially DT tests, which typically have the largest cracks. Intermediate K values are typically obtained with the tests having intermediate crack sizes. Other data also shows K values from fractography being similar to, or being less than, other values [17]. Other data in this review show higher K values for tests in the order listed, e.g. Figs 2 and 4, especially in materials that are known, or expected, to be particularly susceptable to bridging and resultant R-curve effects, e.g. Al_2O_3 and TiB_2, as is the specific demonstration of crack size dependence of K from IF tests [106–108]. This is also implied by the results of Kovar and Readey [3], where strengths of unindented Al_2O_3 samples were less than those of indented samples when G was large enough to expect bridging. Similar trends for higher K with larger starting crack size are also indicated by the more limited data for ceramic composites, i.e. similar or lower K values from fractography [105]. These specific results imply that less, or no, bridging occurred in the unindented strength tests, but some occurred in the indented tests of larger G samples. More generally data indicates little, or no, effect of bridging on normal strength, but increasing effects on γ, K, or S as crack size increases in materials with grain sizes to allow bridging.

The second, and equally important, but much less recognized, issue is that of measuring G. This is typically a very casual and poorly specified procedure. The widely used linear intercept method requires a factor to convert the average intercept to a "true grain" size. Though values of 1.5 or 1.65 are commonly used, there is significant, but uncertain,

TABLE III Ceramic fracture toughness at 22 °C for different tests

D[a]	G[b] (μm)	P[c] (%)	Toughness, K ($MPam^{1/2}$) from[d] F	IF	I	CNB	NB	DT	Investigator(s)
(a) Al_2O_3									
S	5	⩾5		3.4	2.3		4.2–5.5		Lemaitre and Piller [96]
S	< 10	< 5		3.2–4				4.1	Tracy and Quinn [97]
(b) TiB_2									
H	10	2		5.1 ± 0.5				6.7 ± 0.2	Tracy and Quinn [97]
S	8	1		5.5 ± 0.6				8.0 ± 0.3	Tracy and Quinn [97]
(c) SiC									
H	< 1	~ 1–2		3.8 ± 0.3				5.2 ± 0.3	Tracy and Quinn [97]
α-S	4	~ 3–4		3.0 ± 0.1				3.0 ± 0.3	Tracy and Quinn [97]
α-S	–	~ 1–2		2.8	3.0	3.1	4.2		Orange *et al.* [98]
β-S	–	~ 1–2		2.6	3.0	3.4	4.0		Orange *et al.* [98]
α-S	–	~ 2–3		3.3	3.6		4.8		Srinivasan and Seshadri [99]
α-S	5	~ 1–2			3.8		4.6		Seshadri *et al.* [67]
α-S	5		2–3	3.5			4.5–5		Seshadri and Srinivasan [68]
H	–	~ 4		2.6–3.8				3.9	Petrovic and Jacobson [100]
α-S	–	–	3.2						Quinn *et al.* [101]
RS	–	–		3.5 ± 0.4	4.1 ± 0.6			3.8 ± 0.4	Larsen and Walther [102]
(d) Si_3N_4									
RS				2.1 ± 0.1	2.2 ± 0.3			2.1 ± 0.2	Larsen and Walther [102]
H			5.6						Quinn *et al.* [101]
S			3.3						Quinn *et al.* [101]
H	2	~ 0		6.1 ± 0.6	4.0 ± 0.4			5.6 ± 0.9	Larsen and Walther [102]
H				3.5				4.1	Govila [103]
S			6.0 ± 1.6				6.5 ± 1.2		Chakraborty and Mukhopadhyay [104]
S[e]			3.8 ± 0.8				3.9 ± 0.8		Chakraborty and Mukhopadhyay [104]

[a] Mat. = material, Proc. = process; S = sintered, H = hot pressed, RS = reaction sintered.
[b] G = grain size.
[c] P = volume fraction porosity (in % here).
[d] F = fractography, IF = indentation flaw-fracture, I = indentation, CNB = chevron notch beam, NB = notch beam, DT = double torrsion.
[e] SiAlON.

dependence of such factors on grain shape and grain size distribution. Further, the average intercept is often simply given as G, i.e. using a factor of 1, but commonly unstated. Such uncertainties readily vary G by 50–100%. More fundamentally, there are two basic problems with the linear intercept method. First, it is difficult to compare such an average G to the size of an individual grain, as is important in the case of failure initiating from one or a few larger than average grains, which is a frequent occurrence [106–109]. Second, and more fundamental, fracture is an area generating process. Thus, a measure of G reflecting the cross-sectional area of grains, rather than their diameters is more appropriate, and can vary G by a factor of 2 or more [6, 21]. The common variation of G values by ~ 50%, and possibly a few-fold, means the locations and slopes of the various curves shown can vary, and thus may be important in some data differences.

3.2. Toughness–grain size relations

With these above variations in mind, consider the basic K–G trends (Figs 1–8). The trend for distinct K maxima to occur in non-cubic materials is corroborated. This is particularly pronounced for Al_2O_3, where this is now generally attributed to bridging effects. However, the WOF results of Hayashi *et al.* [15] showing sharper maxima at finer G are uncertain in their cause, since the G seems too fine for microcracking. Without bridging the K of Al_2O_3 appears to be approximately constant at ~ 4 $MPa\,m^{1/2}$ over the G range studied, i.e. ~ 1–30 μm. Identification of the specific values at larger G in the absence of bridging is not clear. However, a transition to single crystal or grain boundary K values must begin to occur at larger G [106, 108–110] (Table IV). The three sources of TiO_2 data agree reasonably with one another in that significant K decrease occurs at G beyond 15–20 μm, but the DT values are much higher than the DCB, or WOF values. Some of the differences probably reflect G measurement differences (noted earlier) and stoichiometry differences. The significant K decrease is attributed to substantial microcracking in view of microcracking indicated at $G \sim 20$ μm based on theory and direct observation [39], as well as the drop in E [38]. The K maximum seen in earlier tests is not specifically shown in the more recent tests, but is consistent with them.

Turning now to non-cubic non-oxides, the TiB_2 data clearly shows K decreasing as G increases above ~ 4 μm. This is consistent with this being due to microcracking in view of its greater TEA (three-fold greater than Al_2O_3, as well as greater than EA [111]).

TABLE IV Typical polycrystalline and single crystal fracture toughness at 22°C

Material	Fracture toughness ($MPa\,m^{1/2}$) Single crystal[a]		Polycrystal
Al_2O_3		1.5–2	3.5–4
MgO	{1 0 0}	1	2
TiO_2		0.8	2.5
ThO_2	{1 1 1}	0.65	1.1
Y_2O_3		< 0.9	1.3
ZrO_2		1.3	2.6
$MgAl_2O_4$		1[b]	2
SiC		2	3–4
TiC	{1 0 0}	1.2	3–4

[a] The lowest values, which will dominate fracture. Where cleavage planes are the preferred mode of fracture and are known, they are designated.
[b] Nearly identical for both {1 0 0} and {1 1 0} cleavage [112].

This is supported by E having decreased to half its value at an average G of 24 μm from the value for uncracked material at $G \sim 4$ μm [53]. The G for the indicated K maximum for B_4C and its indicated level (i.e. an increase of 50% or more at the maximum relative to values at finer or larger G) would be consistent with the expectations for non-cubic materials from the current and past non-cubic oxide results since B_4C has very similar TEA, E, and K to Al_2O_3 [65, 11]. However, two factors are puzzling. First, B_4C fracture is typically essentially all transgranular, whereas intergranular fracture, which is commonly an important component of Al_2O_3 fracture over the G range of interest [53], is seen as an important factor in bridging. No bridging observations are known in B_4C. Second and more fundamental is that the above B_4C–Al_2O_3 similarities mean that the location and relative height of the B_4C and Al_2O_3 K peaks should be very similar. The height of the B_4C K maxima are consistent with this, but their G location is low by about an order of magnitude from that expected from a microcracking mechanism. The marked K increase for sintered alpha-SiC is also not certain, but has substantial similarity to results for cubic (beta) SiC and MgO discussed below.

Turning to cubic materials, there are some results consistent with previous data and expectations, and some that are different. Thus, oxide and ZnS data again show little or no dependence on G relative to non-cubic materials such as Al_2O_3 (but the limited scatter of the ZnS data makes its maximum statistically significant). The occurrence of a K maximum is more clearly indicated for Y_2O_3 by added data (though the reasons for the higher level of Tani *et al.*'s data [48] is not clear). Again, the decrease in K at large G may reflect the transition to single crystal (Table III) or grain boundary (i.e. bicrystal) K values, which may be half or less than the single crystal values. However, the cause(s) of the definitive K maxima shown in two studies of mainly, or exclusively, cubic SiC is uncertain, as is the rise in K of sintered alpha-SiC noted above, which would also be consistent with a K maximum, but at larger G. None of these SiC data are obviously inconsistent with other SiC data, e.g. of the earlier survey due to data scatter and more limited number and extent of grain sizes measured. Possible effects of the presence of some non-cubic (alpha) SiC do not appear to be a viable explanation for these variations since the TEA and EA of alpha-SiC are modest [11]. Since maxima were indicated for two very different processing methods, it is unlikely to be an artifact of processing.

Whether the cubic materials K maxima are intrinsic, e.g. reflecting effects of EA, or extrinsic, e.g. reflecting more residual grain boundary impurities or porosity, is not clear. However, four factors may singly, or collectively, contribute to, or be the cause of, at least some of, the K maxima. One of the most general is limited porosity, as shown by the MgO data (Fig. 4). This is likely to be an important factor in the sintered alpha-SiC, since it has at least a few per cent P, which also most likely decreases in content and shifts to more intragranular porosity as G increases, as in MgO. This may also be a factor in the B_4C increase at fine G (and possibly the high K at larger G, as noted earlier) since these bodies had up to a few per cent P. Second, are changes of stoichiometry, and grain orientation that often accompany grain size changes, especially in CVD materials. Third, for indent derived values, these may reflect indent cracking deviations. A recent study of hardness shows that substantial cracking, often of a spalling character along grain boundaries, increasingly occurs around indents as the indent size approaches the grain size [94]. Such cracking, which leads to hardness minima, is in addition to, and some may be instead of, the cracks used in determining toughness, but could alter, most likely increase, resultant K values. This could thus be a source of some, most likely, more modest K maxima, but would be dependent on the indent load and type. It also is not necessarily universal, i.e. this added indent cracking was not observed with Y_2O_3 hardness indents, and thus may not be applicable to the Y_2O_3 data (Fig. 4). However it is also significantly enhanced by grain boundary phases, and so can be variable for a given material, as well as indent load and geometry. Such indent-cracking is most likely a factor in the K maxima of ZnS, and may be a factor in that of CVD SiC; other maxima appear at too small a G value to be due to this mechanism. However, the B_4C K maxima are associated with hardness maxima, not minima. Fourth, crack bridging, e.g. due in part to EA, may be a factor. The lower maxima levels could reflect less bridging associated with the common occurrence of significant transgranular fracture, and variations could reflect variations in fracture mode with grain boundary phases. Thus, the source of some of the maxima are known or suspected, but many are unknown and can only be resolved by more study of the specific materials, processes, and test techniques. However, it is also important to compare the K results with those for strength. While this is the focus of another paper [4], some key points are outlined below.

3.3. Strength–toughness, toughness–porosity, and crack bridging

The K maxima as a function of G, especially the more pronounced ones mainly for non-cubic materials, are quite inconsistent with the G dependence of strength [4–9] for almost all bodies. Strength almost invariably shows a continuous decrease, i.e. no maximum, with increasing G. The only clear exception is the strength of the polycarbosilane derived SiC, which shows a similar, but somewhat less pronounced strength maxima similar to that for K (Fig. 8). The increase in strength of sintered alpha-SiC (Fig. 8) is much less than that of its K, and is most likely an artifact of the changing porosity expected in this material as discussed above for its K. Thus, correction of the alpha-SiC strength for P is expected to give strength decreasing with increasing G, as broadly found for bodies of constant P, especially $P = 0$ [5–9].

The greater S–G versus K–G decrease of TiB_2 (Fig. 7) probably reflects the substantial G distribution in the bodies studied, and the greater sensitivity of S to this. While this shows the need for detailed evaluation of S–G and K–G effects, there are other S–K differences, often much more pronounced than the TiB_2 differences shown in Fig. 7. Thus, S variations do not necessarily reflect the significant K differences for TiO_2 (Fig. 3) and Y_2O_3 (Fig. 4) [7]. Also, while the trends for K maxima of composites observed as a function of the amount of dispersed particulates and whiskers often agree with strength trends, there are also serious S–K discrepancies for composites similar to those observed here, and discussed in more detail elsewhere [4].

The P dependence of γ and K shows as much or more deviation from normal S and E dependence as does G dependence. However, the deviations from the normal S–P or E–P behaviour, and the suggested bridging, provide an explanation for porous materials having such improved resistance to severe thermal shock. These γ–P, K–P deviations, and the suggested bridging appears to be a fruitful area for research.

For both the G and P dependence of S the least, or no, discrepancy with γ and K tests occurs when the crack size in the latter is similar to that controlling strength. While it might be argued that S and K values calculated from them based on fractography are not truly independent results since the latter involves the former, two factors should be noted. First, for all bodies this involves another key set of observations and measurements, namely of the flaw size, geometry, and location. Second, for porous bodies the P dependence of the resulting K generally agrees with that of both S and E. Thus, K values from fractography are generally consistent and those from indentation fracture, often the next closest. Values of K from tests involving substantial R-curve effects are the least consistent with strength behaviour.

Finally, the issue of the pertinence of bridging effects on K to normal strengths has not been adequately addressed [110]. Fractography is an important tool that should be applicable to many occurrences of bridging. However there are many other sources of questions of the pertinence of bridging and wake phenomena to strength that are also tools to resolve these issues. An important one of these is comparison of the microstructural dependence of S, K, γ and E. This paper is a component of such comparison. Strengths are normally controlled by flaws that accelerate to failure and are commonly orders of magnitude smaller than the large, arresting cracks used in bridging studies. (It should be noted that the recent trend to refer to the "long" and "short" regions of crack growth is misleading since the critical issue is not just the length of the crack into the material but also in the perpendicular dimension, i.e. the crack area relative to that of the strength controlling microstructure, which also depends on the lateral dimension of the crack, not just how deeply it is propagated along the sample.)

4. Summary and conclusions

The grain size dependencies of γ and K often show substantial maxima. Many of these maxima appear to correlate with bridging and associated R-curve behaviour in most testing of non-cubic oxides such as Al_2O_3, where most maxima correlate with microcracking from stresses resulting from thermal expansion anisotropy (TEA) of the crystalline grains. However, some maxima, e.g. that observed for B_4C, are very inconsistent in association with TEA since the G of the maxima are far too small, e.g. by a factor of 10 or more.

Lesser, but often definitive maxima of γ and K as a function of G are also shown for some cubic materials. Results for other cubic materials are not inconsistent with such maxima, but may simply entail data at too few grain sizes. The γ and K maxima are generally inconsistent with S for both cubic and non-cubic materials.

The porosity dependence of γ and K show continuous decreases with increasing P in some cases similar to that for strength and E. However, a substantially lower rate of decrease is often found, including no decrease, or a temporary halt to the normal decrease of γ and K_{IC} with increasing P are observed. The latter may entail a temporary increase of γ or K with increasing P over a limited P range. These deviations from the normal decrease with increasing P appear to be associated with bridging, but are variable in the extent and P range in which they occur. This appears to depend on the character of the porosity, and possibly on interaction of this with the amount of porosity and the test. These effects of P on γ and K are cited as a probable reason for the frequent improvement in the resistance to failure from substantial thermal shock in porous bodies. Thus, further study of the P effects on γ and K should be a fruitful area for research.

The G and P dependence of γ and K show significant discrepancies with strength behaviour, which are considered in more detail in a companion paper [4].

References

1. K. KENDALL, N. McN. ALFORD, S. R. TAN and J. D. BIRCHALL, *J. Mater. Res.* **1** (1986) 120.
2. R. W. RICE, *Ceram. Eng. Sci. Proc.* **11** (1990) 667.
3. D. KOVAR and M. J. READEY, *J. Amer. Ceram. Soc.* **77** (1994) 1928.
4. R. W. RICE, to be published.
5. R. W. RICE, in "The Science of Ceramic Machining and Surface Finishing II", NBS, Special Publication 562, edited by B. J. Hockey and R. W. Rice (U.S. Government Printing Office, Washington, D.C., 1979) pp. 429–54.
6. R. W. RICE, to be published.
7. R. W. RICE, to be published.
8. R. W. RICE, to be published.
9. R. W. RICE, in "Treatise on Materials Science and Technology", Vol. 11, Properties and Microstructure, edited by R. K. MacCrone (Academic Press, New York, 1977) pp. 191–381.
10. R. W. RICE, to be published.
11. R. W. RICE, to be published.
12. R. W. RICE, S. W. FREIMAN, and P. F. BECHER, *J. Amer. Ceram. Soc.* **64** (1981) 345.
13. R. W. RICE, "Fracture Mechanics Methods for Ceramics, Rocks, and Concrete" edited by S. W. Freiman and E. R. Fuller Jr ASTM STP 745 (American Society for Testing Materials, Philadelphia, PA, 1982) pp. 96–117.
14. R. W. RICE and S. W. FREIMAN, in Ceramic Microstructures '76: With Emphasis on Energy Related Applications, University of California, Berkley, CA, 24–27 August, 1976, edited by R. M. Fulrath and J. A. Pask (Westview Press, Bolder, Colorado, 1977) pp. 800–23.
15. K. HAYASHI, Y. TATEWAKI, S. OZAKI and T. NISHIKAWA, *J. Ceram. Soc. Jpn. Int. Ed.* **96** (1988) 516.
16. R. W. RICE, R. C. POHANKA and W. J. McDONOUGH, *J. Amer. Ceram. Soc.* **63** (1980) 703.
17. R. W. RICE, in "Ceramic Transactions", Vol. 17, Fractography of Glasses and Ceramics II, edited by V. D. Frechette and J. R. Varner (American Ceramic Society, Westerville, Ohio, 1991) pp. 509–45.
18. R. W. RICE, *J. Amer. Ceram. Soc.* **77** (1994) 2232.
19. R. W. RICE and S. W. FREIMAN, *ibid.* **64** (1981) 350.
20. N. CLAUSSEN, R. MUSSLER and M. V. SWAIN, *ibid.* **65** (1982) C14.
21. B. MUSSLER, M. V. SWAIN and N. CLAUSSEN, *ibid.* **65** (1982) 566.
22. A. T. YOKOBORI Jr., T. ADACHI and T. YOKOBORI, in Advances in Electronic Packaging 1992, Vol. 2, Materials and Process Reliability, Quality Control and NDE, edited W. T. Chen and H. Abe, American Society for Mechanical Engineers, New York, 1992) pp. 739–43.
23. K. HAYASHI, K. GOTOH and T. NISHIKAWA, *J. Ceram. Soc. Jpn Int. Ed.* **99** (1991) 604.
24. D. MUNZ, R. T. BUBSEY and J. L. SHANNON Jr., *J. Amer. Ceram. Soc.* **63** (1980) 300.
25. T. NISHIDA, Y. HANAKI and G. PEZZOTTI, *ibid.* **77** (1994) 606.
26. Z. D. YANG, Y. Y. WU and K. CHEN, in "Ceramic Materials and Components for Engines", Proceedings of the 2nd International Symposium, Lübeck-Travemünde, FRG, 14–17 Aprl, 1986, edited by W. Bunk and H. Hausner (Verlag Deutsche Ker. Gesl., 1986) pp. 559–56.
27. S. SCLOSA, D. F. DAILLY and G. W. HASTINGS, *Trans. J. Br. Ceram. Soc.* **81** (1982) 148.
28. H. HÜBER and W. JILLET, *J. Mater. Sci.* **12** (1977) 117.
29. J. D. B. VELDKAMP and N. HATTU, *Phillips J. Res.* **34** (1979) 1.
30. R. W. STEINBRECH and O. SCHMENKEL, *J. Amer. Ceram. Soc.* **71** (1988) C271.
31. G. VEKINS, M. F. ASHBY and P. W. R. BEAUMONT, *Acta Metals Mater.* **38** (1990) 1151.
32. D. BLEISE and R. W. STEINBRECH, *J. Amer. Ceram. Soc.* **77** (1994) 315.
33. P. CHANTIKUL, S. J. BENNISON and B. R. LAWN, *ibid.* **73** (1990) 2419.
34. C. CM. WU, R. W. RICE and P. F. BECHER, in "Fracture Mechanics Methods for Ceramics, Rocks, and Concrete", edited by S. W. Freiman and E. R. Fuller Jr., ASTM STP 745 (American Society for Testing Materials, Philadelphia, PA, 1982) pp. 127–40.
35. J. J. CLEVELAND, MSc thesis, Pennsylvania State University (1977).
36. R. C. POHANKA, S. W. FREIMAN, K. OKAZAKI and S. TASHIRO, in "Fracture Mechanics of Ceramics", Vol. 5, edited by R. C. Bradt, A. G. Evans, D. P. H. Hasselman, and F. F. Lange (Plenum Press, New York, 1983) pp. 353–64.
37. W. P. MINNEAR and R. C. BRADT, *J. Amer. Ceram Soc.* **63** (1980) 485.
38. K. YASUDA, S. OHSAWA, Y. MATSUO and S. KIMURA, *J. Jpn. Soc. Mater. Sci.* **41** (1992) 482.
39. R. W. RICE and R. C. POHANKA, *J. Amer. Ceram. Soc.* **62** (1979) 559.
40. J. B. KESSLER, J. E. RITTER Jr. and R. W. RICE, in "Materials Science Research", Vol. 7, Surfaces and Interfaces of Glass and Ceramics, edited by V. D. Frechette, W. C. LaCourse, and V. L. Burdick (Plenum Press., New York, 1974) pp. 529–44.
41. K. YASUDA, S.-D. KIM, Y. KANEMICHI, Y. MATSUO and S. KIMURA, *J. Ceram. Soc. Jpn Int. Ed.* **98** (1990) 1110.
42. K. YASUDA, Y. TSURU, Y. KANEMICHI, Y. MATSUO and S. KIMURA, *ibid.* **100** (1992) 790.
43. Y. TSURU, K. YASUDA, Y. MATSUO, S. KIMURA and E. YASUDA, *ibid.* **101** (1993) 165.
44. K. YASUDA, Y. TSURU, Y. MATSUO, S. KIMURA and T. YANO, *ibid.* **101** (1993) 648.
45. J. J. MECHOLSKY JUN., S. W. FREIMAN and R. W. RICE, *J. Mater. Sci.* **11** (1976) 1310.
46. L. D. MONROE and J. R. SMYTH, *J. Amer. Ceram. Soc.* **61** (1978) 538.
47. W. H. RHODES, J. G. BALDONI and G. C. WEI, GTE Laboratory Final Report for ONR contract N00014-82-C-0452, July (1986).
48. T. TANI, Y. MIYAMATO, M. KOIZUMI and M. SHIMADO, *Ceram. Int.* **12** (1986) 33.
49. A. GHOSH, K. W. WHITE M. G. JENKINS, A. S. KOBAYASHI and R. C. BRADT, *J. Amer. Ceram. Soc.* **74** (1991) 1624.
50. K. W. WHITE and G. P. KELKAR, *ibid.* **74** (1991) 1732.
51. *Idem, ibid.* **75** (1992) 334.
52. R. L. STUART, M. IWASA and R. C. BRADT, *ibid.* **64** (1981) C22.
53. R. W. RICE, in "Fractography of Glasses and Ceramics III", edited by J. R. Varner and G. Quinn (American Ceramic Society, Westerville, OH) in press.
54. H. R. BAUMGARTNER and R. A. STEIGER, *J. Amer. Ceram. Soc.* **67** (1984) 207.
55. M. K. FERBER, P. F. BECHER and C. B. FINCH, *ibid.* **74** (1983) C2.
56. P. F. BECHER, C. B. FINCH and M. K. FERBER, *J. Mater. Sci. Lett.* **5** (1986) 195.
57. E. S. KANG, C. W. JANG, C. H. LEE and C. H. KIM, Densification and Mechanical Properties of Titanium Diboride Ceramics, *J. Amer. Ceram. Soc.* **72** (1989) 1868.
58. J. MATSUSHITA, H. NAGGASHIMA and H. SAITO, *J. Ceram. Soc. Jpn Int. Ed.* **99** (1991) 77.
59. R. W. RICE, K. R. MCKINNEY and C. CM. WU, Unpublished data.
60. A. A. KORNEEV, I. T. STAPENKO, M. A. DOLZHEK, A. G. MIRONOVA, N. D. RYBALCHENKO, I. A. LYASHENKO and V. P. PODTYKAN, *Poroshkovaya Metall.* **349** (1992) 69 (in Russian).
61. K. NIIHARA, *Amer. Ceram. Soc. Bull.* **63** (1984) 1160.
62. K. NIIHARA, A. NAKAHIRA and T. HIRAI, *J. Amer. Ceram. Soc.* **74** (1884) C13.
63. D. KALISH, E. V. CLOUGHERTY and J. RYAN, Manlabs, Inc. Final Report for U.S. Army Materials Research Laboratory Contract DA-19-066-AMC-283(x), November (1966).
64. R. W. RICE, C. CM. WU and F. BORCHELT, *J. Amer. Ceram. Soc.* **77** (1994) 2539.
65. R. W. RICE, *ibid.* **73** (1990) 3116.

66. H. KODAMA and T. MIYOSHI, *ibid.* **73** (1990) 3081.
67. S. G. SESHADRI, M. SRINIVASAN and K. Y. CHIA, in Silicon Carbide '87, Ceramic. Transactions, Vol 2, edited by J. D. Cawley and C. E. Semler (Am. Cer. Soc., Westerville, OH., 1989) pp. 215–26.
68. S. G. SESHADRI and M. SRINIVASAN, *J. Amer. Ceram. Soc.* **64** (1981) C69.
69. T. OHJI, Y. YAMAUCHI, W. KANEMATSU and S. ITO, *ibid.* **72** (1989) 688.
70. A. K. MUKHOPDHAY, D. CHAKRBORTY and J. MUKERJI, *J. Mater. Sci. Lett.* **6** (1987) 1198.
71. R. K. GOVILA, *J. Mater. Sci.* **23** (1988) 1141.
72. R. W. RICE, K. R. MCKINNEY, C. CM. WU, S. W. FREIMAN and W. J. McDONOUGH, *ibid.* **20** (1985) 1392.
73. J. A. SALEM, S. R. CHOI, M. R. FREEDMAN and M. G. JENKINS, *ibid.* **27** (1992) 4421.
74. C.-W. LI, D. J. LEE and S.-C. LUI, *J. Amer. Ceram. Soc.* **75** (1992) 1777–85.
75. T. KAWASHIMA, H. OKAMOTO, H. YAMAMOTO and A. KITAMURA, *J. Ceram Soc. Jpn Int. Ed.* **99** (1991) 310.
76. N. HIROSAKI, Y. AKIMUNE and M. MITOMO, *J. Amer. Ceram. Soc.* **76** (1993) 1892.
77. K. MATSUHIRO and T. TAKAHASHI, *Ceram. Eng. Sci. Proc.* **10** (1989) 807.
77a. C. M. B. HENDERSON and D. TAYLOR, *Trans. J. Br. Ceram. Soc.* **74** (1975) 49.
78. D. TOWNSEND and J. E. FIELD, *J. Mater. Sci.* **25** (1990) 1347.
79. D. C. C. LAM, F. F. LANGE and A. G. EVANS, *J. Amer. Ceram. Soc.* **77** (1994) 2113.
80. C. CM. WU and R. W. RICE, *Ceram. Eng. Sci. Proc.* **6** (1985) 977.
81. J. A. CAPPOLA and R. C. BRADT, *J. Amer. Ceram. Soc.* **56** (1973) 392.
82. R. F. PABST, in "Fracture Mechanics of Ceramics", Vol. 2, edited by R. C. Bradt, D. P. H. Hasselman, and F. F. Lange (Plenum Press, New York, 1974) pp. 555–65.
83. N. CLAUSSEN, R. PABST and C. P. LAHMANN, *Proc. Br. Ceram. Soc.* **25** (1975) 139.
84. A. G. EVANS and G. TAPPIN, *ibid.* **20** (1972) 275.
85. D. R. BISWAS and R. M. FULRATH, *Trans. J. Br. Ceram. Soc.* **79** (1980) 1.
86. G. W. HOLLENBURG and G. WALTHER, *J. Amer. Ceram. Soc.*, **63** (1980) 610.
87. YU. L. KRASULIN, V. N. TIMOFEE, S. M. BARINOV and A. B. IVANOV, *J. Mater. Sci.* **15** (1980) 1402.
88. R. W. RICE, *ibid.* **19** (1984) 895.
89. E. D. CASE and J. R. SMYTH, *ibid.* **16** (1981) 3215.
90. F. J. P. CLARKE, H. G. TATTERSALL and G. TAPPIN, *Proc. Br. Ceram. Soc.* **6** (1966) 163.
91. A. D. OSIPOV, I. T. OSTAPENKO, V. P. PODTYKAN, N. S. POLTAVSEV and I. A. SNEZHKO, *Poroshkovaya Metall.* **322** (1989) 48 (in Russian).
92. K. R. McKINNEY and R. W. RICE, in "Fracture Mechanics Methods for Ceramics, Rocks and Concrete", ASTM STP 745, edited by S. W. Freiman and E. R. Fuller Jr. (American Society for Testing Materials, Philadelphia, PA, 1981) pp. 118–26.
93. R. P. INGEL, Private communication.
94. R. W. RICE, C. CM. WU and F. BORCHELT, *J. Amer. Ceram. Soc.* **77** (1994) 2539.
95. R. W. RICE, *ibid.* **77** (1994) 2479.
96. P. LEMAITRE and R. PILLER, *J. Mater. Sci. Lett.* **7** (1988) 772.
97. C. A. TRACY and G. D. QUINN, *Ceram. Eng. Sci. Proc.* **15** (1994) 837.
98. G. ORANGE, H. TANAKA and G. FANTOZZI, *Ceram Int.* **13** (1987) 159.
99. M. SRINIVASAN and S. G. SESHADRI, "Fracture Mechanics of Ceramics, Rocks and Concrete", ASTM STP 745, edited by S. W. Freiman and E. R. Fuller Jr. (American Society for Testing Materials, Philadelphia, PA, 1981) pp. 46–48.
100. J. J. PETROVIC and L. A. JACOBSON, *J. Amer. Ceram. Soc.* **59** (1976) 34.
101. G. D. QUINN, D. R. MESSIER and L. L. SCHOILER, Army Materials Laboratory Report, AMMRCC TR 83-18.
102. D. C. LARSEN and G. C. WALTHER, Itt Research Institute Semiannual Interim Technical Report No. 6 for Air Force Contract F33615-75-C-5196, 7/20/1978.
103. R. K. GOVILA, *J. Amer. Ceram. Soc.* **65** (1980) 319.
104. D. CHAKRABORTY and A. K. MUKHOPADHYAY, *Central Glass Ceram. Bull* **34** (1987) 59.
105. R. W. RICE, *Ceram. Eng. Sci. Proc.* **11** (1990) 667.
106. R. W. RICE, S. W. FREIMAN and J. J. MECHOLSKY Jr., *J. Amer. Ceram. Soc.* **63** (1980) 129.
107. J. A. CAPPOLA and R. C. BRADT, *ibid.* **55** (1972) 455.
108. R. W. RICE, in "Treatise on Materials Science and Technology", Vol. 11, Properties and Microstructure, edited by R. K. MacCrone (Academic Press, New York, 1977) pp. 191–381.
109. *Idem*, to be published.
110. *Idem, J. Amer. Ceram. Soc.* **76** (1993) 1898.
111. *Idem, J. Mater. Sci. Lett.* **13** (1994) 1261.
112. R. W. RICE, C. CM. WU and K. R. McKINNEY, *J. Mater. Sci.* submitted.

Received 3 October
and accepted 20 November 1995